

# Coherent Vector Meson Photo-Production from Deuterium at Intermediate Energies

T.C. Rogers<sup>a</sup>, M.M. Sargsian<sup>b</sup>, M.I. Strikman<sup>a\*</sup>

<sup>a</sup>*Department of Physics,  
Pennsylvania State University,  
University Park, PA 16802, USA*

<sup>b</sup>*Department of Physics,  
Florida International University,  
Miami, FL 33199*

(Dated: May 16, 2019)

## Abstract

We analyze the cross section for vector meson photo-production off a deuteron for photon energies in the intermediate range just above threshold. We reproduce the steps in the derivation of the conventional non-relativistic Glauber expression based on an effective covariant diagrammatic method while making corrections for Fermi motion and near threshold kinematic effects. We show that, just above the threshold for vector meson production, the usual Glauber factorization breaks down and we derive corrections to the usual Glauber method to linear order in longitudinal nucleon momentum. The purpose of our analysis is to establish methods for probing interesting physics in the production mechanism for  $\phi$ -mesons and heavier vector mesons. The framework which we derive for dealing with near threshold effects also tests the consistency of usual non-relativistic methods and the vector meson dominance hypothesis in the sensitive kinematical region just above threshold. We demonstrate how neglecting the breakdown of Glauber factorization can lead to an over estimate of basic cross sections extracted from nuclear data.

Keywords: Vector Meson Dominance, Phenomenological Models

---

\*E-mail: rogers@phys.psu.edu

## I. INTRODUCTION

Coherent vector meson production from nuclei has proven to be a useful tool for studying the structure of vector mesons. In the high energy, small angle scattering regime, well above the threshold for vector meson production, the large volume of available experimental data involving proton targets consistently supports the validity of the vector meson dominance (VMD) model for small photon virtualities [1, 2]. This, combined with the onset of the eikonal regime in the diffractive region has lead to the development of a successful theoretical framework for the description of vector meson photo-production off nuclei based on the combined VMD model and Glauber theory of hadron-nuclei rescattering [1, 3]. The simplicity of the VMD-Glauber framework arises from the fact that at high energies the basic  $\gamma N \rightarrow VN$  and  $VN \rightarrow NN$  amplitudes vary slowly with the total energy of the  $\gamma N$  system relative to the range of important energies in the deuteron wavefunction. This observation leads to the factorizability of the basic  $\gamma N \rightarrow VN$  amplitude from the momentum space integral, and yields the conventional Glauber multiple scattering series consisting of non-relativistic form factors and elementary scattering amplitudes.

The VMD-Glauber theory has lead, in particular, to the demonstration that the coherent photo-production of vector mesons off the deuteron at large  $-t$  is defined mainly by the rescattering contribution [4]. Since the  $VN \rightarrow VN$  amplitude appears in the double scattering term, one may use nuclear photo-production reactions to study the properties of vector mesons [5]. By choosing different  $t$ , one can control the relative distance at which rescattering may occur, and allows one to investigate the space-time evolution of hadronic systems produced in electro(photo)- production.

An extension of the above program is the study of coherent vector electro-production at large  $Q^2$ . In this case, coherent vector meson production from the deuteron can be used to study color coherence/transparency phenomena in vector meson electro-production at high  $Q^2$ . The onset of color transparency will reveal itself through the substantial drop in the double scattering contribution with an increase of  $Q^2$  as opposed to the nearly energy independent behavior of the double scattering term for the generalized VMD prediction [5].

In this paper we consider yet another venue of application for vector meson photo-production off nuclear targets by considering photo-production in the intermediate range of energies just above the threshold. These reactions have great potential for probing sev-

eral effects such as non-diffractive, OZI violating mechanisms for vector meson production mesons, in-medium modifications of vector mesons, the importance of “non-ideal”  $\omega - \phi$  mixing, and other new mechanisms for vector meson production (see Refs. [6, 7, 8]).

Finally, it would be interesting to learn whether the  $\phi$ -meson is produced with a small enough transverse size that quark degrees of freedom may become relevant, as in the case of  $J/\psi$ -production. Actually, in the case of  $J/\psi$ , the cross section of the  $J/\psi - N$  interaction  $\sigma_{J/\psi-N} \sim 3 mb$ , [9] estimated based on the A-dependence of  $J/\psi$  photo-production at energies  $\sim 20$  GeV, is much larger than the estimate based on the VDM:  $\lesssim 1 mb$ . This is likely due to the color transparency phenomenon [9].

The interest in intermediate energy reactions makes it necessary to re-evaluate the assumptions of the traditional Glauber series method, and to develop a new theoretical approach. This paper addresses the issues one must face when considering photon energies large enough that the eikonal approximation ( $\gtrsim 1$  GeV) is an appropriate description of hadronic reinteractions, but not large enough that it is appropriate to neglect vector meson masses in kinematical calculations or the non-trivial s-dependence of the amplitude for photo-production of vector mesons from the nucleon. Furthermore, for small photon energies ( $\lesssim 3$  GeV) the VMD hypothesis becomes suspect as a description of the  $\gamma N \rightarrow VN$  amplitude, so we restrict ourselves to arbitrary photon-nucleon amplitudes. Jlab has produced data for  $J/\psi$  production that is currently being analyzed.

Although we retain the eikonal approximation, our approach is distinctly different from the usual Glauber-VMD approach. In particular, one of the basic assumptions used in the Glauber approach is that the basic  $\gamma N \rightarrow VN$  and  $VN \rightarrow VN$  cross sections are slowly varying functions of center of mass energy and that the small Fermi momentum of the nucleons can be neglected in the evaluation of the total energy of the  $\gamma N$  and  $VN$  systems. These assumptions result in the usual factorizability already discussed above. Near the threshold energy, however, the photon energy is comparable to the vector meson mass, and the basic amplitude gains non-trivial energy dependence from a precise accounting of kinematics. Moreover, the usual smooth rise in the total  $\gamma N \rightarrow VN$  cross section characteristic of high energy diffractive scattering is absent at lower energies. Fermi motion effects thereby destroy the factorizability of nuclear scattering into basic amplitudes and form factors. That such problems with factorizability may arise has been no for a long time [1]. Also, the longitudinal momentum transfer (proportional to  $M_V^2/E_\gamma$ ) play an important role as com-

pared to reactions in the diffractive regime and further calls into question the factorization hypothesis.

In this paper we are specifically interested in near threshold coherent photo-production of vector mesons off a deuteron target. The kinematics under consideration are such that the produced vector mesons are energetic enough for the eikonal approximation to be valid. However the energy dependence of the  $\gamma N \rightarrow VN$  amplitude due to the nearness to threshold will require that we account for Fermi motion effects which, in turn, requires that account for non-factorization effects. In the derivation of the total  $\gamma D \rightarrow VD$  amplitude we use the generalized eikonal approximation [10, 11] which allows us to derive the scattering amplitudes starting with corresponding effective Feynman diagrams.

By maintaining the result in terms of momentum space integrals, both longitudinal and Fermi motion effects may be explicitly taken into account consistently. In our derivations, we keep only the corrections to the basic amplitudes that are of linear order in longitudinal exchanged momentum or nucleon momentum (neglecting order  $\mathbf{p}^2/m_N^2$  corrections, where  $\mathbf{p}$  is the bound state nucleon momentum). This allows us to relate  $D \rightarrow NN$  transition vertex to the nonrelativistic wave function of the deuteron.

We also note that the basic amplitude for  $\gamma N \rightarrow VN$  scattering is obtained directly from experimental data with a nucleon target. The secondary scattering amplitude is usually determined from the VMD hypothesis at high energies, but the use of VMD is suspect near threshold. However, the validity of the GEA implies that the intermediate vector meson is nearly on-shell. Hence, fitting data to our modified Glauber theory just above the threshold by using the  $VN \rightarrow VN$  amplitude as a parameter allows one to determine a value for the  $VN \rightarrow VN$  cross section.

The paper is organized as follows: In Sec. II we derive scattering amplitudes for the  $\gamma D \rightarrow VD$  reaction based on the generalized eikonal approximation. In Sec. III we compare our results at near threshold kinematics with the prediction of conventional VMD-Glauber theory. We identify the effects which are most responsible for the divergence of the our prediction from the Glauber theory. We demonstrate that effects calculated in this paper, if unaccounted for, can yield a misinterpretation of the  $VN$  scattering cross section as it is extracted from the data using Glauber approximation. In Sec. IV we present some sample calculations and we end with a summary and conclusions. In the Appendices we discuss the details of the derivations, as well as demonstrate the convergence of our approach to the

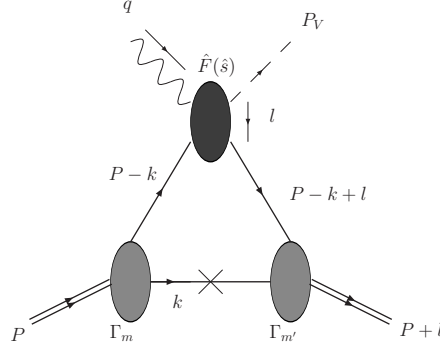


FIG. 1: The impulse diagram for photo-production. The cross on the spectator nucleon line indicates that the spectator nucleon will be taken on shell in the non-relativistic approximation. (For all Feynman graphs we use Jaxodraw [12].)

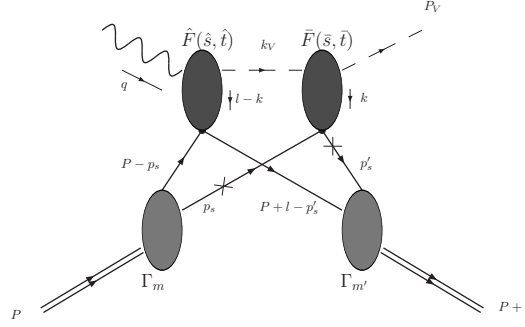


FIG. 2: The double scattering diagram for photo-production.

conventional Glauber theory.

## II. THE CROSS SECTION CALCULATION

### A. Reaction and Kinematics

We study the coherent photo-production of vector mesons off the deuteron in the reaction:

$$\gamma + D \rightarrow V + D', \quad (1)$$

where  $P \equiv (M_D, 0)$  and  $P' \equiv (E_D, \mathbf{P}')$  define the initial and final four momenta of the deuteron. We use natural units ( $c = \hbar = 1$ ). The relevant effective Feynman graphs in the eikonal approximation are shown in Figs. 1 and 2.  $q \equiv (E_\gamma, \mathbf{q})$  and  $P_V \equiv (E_V, \mathbf{P}_V)$

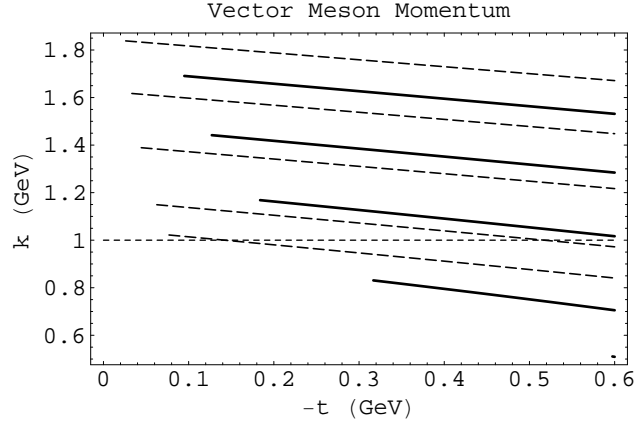


FIG. 3: Produced vector meson 3-momentum as a function of  $-t$  for a given set of fixed  $E_\gamma$ . The solid lines correspond to  $\phi$ -meson production, whereas the dashed lines correspond to  $\rho^0$ -meson production. The photon energies in each case, going from the bottom curve to the top curve are 1.3, 1.4, 1.6, 1.8, 2.0 GeV.

define the 4-momenta of the initial photon and the final state meson respectively. The three-momentum transferred is defined as  $\mathbf{l} = \mathbf{q} - \mathbf{P}_V$ . In our calculations we concentrate on near threshold kinematics, but chosen at values of  $-t$  so that the final state vector meson 3-momentum is of order  $\gtrsim 1$  GeV. This allows us to use the eikonal approximation in treating the rescattering of the outgoing vector meson.

Fig. 3 shows the the lab frame 3-momentum of the final state vector meson as a function of  $-t$  for a set of incident photon energies in the vicinity of threshold for the case of  $\rho^0$  and  $\phi$ -meson production. We see that, as the photon energy increases, the eikonal regime is quickly approached at small  $-t$ . This demonstrates that it is possible, even in the near threshold region, to apply the eikonal approximation to the reaction of Eq.(1) so long as the 3-momentum of the final state vector meson is chosen appropriately.

We assume that the non-relativistic model of the  $N - N$  interaction can be represented by a  $D \rightarrow NN$  vertex. Furthermore, assuming that we are working in the eikonal regime we base our derivations on the Generalized Eikonal Approximation (GEA) which allows one to organize our calculation around a set of effective Feynman rules, expanded in terms of the number of rescatterings. For the reaction of Eq.(1) there are only two relevant diagrams: the single scattering diagram (Born term) of Fig. 1 and the double scattering diagram of Fig. 2.

As illustrated in Fig. 2, the double scattering term has two distinct interaction vertices. The vector meson is produced at the first vertex and rescatters from the second. In this it is reminiscent of nucleon knock-out reactions, in which a fast nucleon is knocked out at the first vertex and then rescatters from spectator nucleons. The fact that, as Fig. 3 demonstrates, the intermediate vector meson carries high momentum, even relatively near to threshold, is essential since it allows us to use the GEA approach to calculate the scattering amplitudes corresponding to the diagrams in Fig 1 and Fig. 2.

## B. The Born Amplitude

We start with the calculation of the amplitude corresponding to the Born term of Fig. 1.  $F_{m,m'}^0(s,t)$  will denote the  $\gamma D \rightarrow VD$  scattering amplitude for the Born term in which only one of the nucleons takes part in the interaction, whereas  $\hat{F}(\hat{s},t)$  will denote the basic  $\gamma N \rightarrow VN$  scattering amplitude. A hat on a variable indicates that it is associated with the  $\gamma N \rightarrow VN$  subprocess rather than the process of Eq. (1). The superscript, 0, is meant to distinguish this term from the double scattering term. The initial and final polarizations of the deuteron are denoted by  $m$  and  $m'$  respectively. Because of the nearness to threshold, the  $\hat{F}(\hat{s},t)$  amplitude is not necessarily diffractive and we do not assume the validity of the VMD hypothesis. We neglect the spin-flip component of the basic amplitude (i.e.  $\hat{F}$  and  $\bar{F}$  are approximately diagonal in nucleon spin.) The  $D \rightarrow NN$  vertex is denoted by  $\Gamma_m$ . For simplicity, information on the spin structure is absorbed into  $\Gamma_m$ . All variables correspond to the labels in the Feynman diagram of Fig. 1 for the single scattering (Born) term. The free nucleon mass is denoted by  $m_N$ .

By applying effective Feynman rules to the graph in Fig. 1 we obtain the manifestly covariant scattering amplitude,

$$\begin{aligned}
F_{m,m'}^0(s,t) &= - \int \frac{d^4\mathbf{k}}{i(2\pi)^4} \frac{\Gamma_m^\dagger(P-k+l)\hat{F}(\hat{s},t)\Gamma_m(P-k)}{[(P-k+l)^2 - m_N^2 + i\epsilon][(P-k)^2 - m_N^2 + i\epsilon][k^2 - m_N^2 + i\epsilon]} \quad (2) \\
&+ (p \leftrightarrow n).
\end{aligned}$$

$(p \leftrightarrow n)$  refers to the term in which the neutron and proton are inverted. In the remainder of this text, Mandelstam variables that appear within an integral are understood to be functions of internal nucleon 4-momentum and the incident photon 4-momentum.

We proceed with the derivation by estimating the loop integral in Eq.(2) up to terms of order  $\frac{\mathbf{k}^2}{m_N^2}$ . This approximation allows us to evaluate the integral in Eq.(2) by keeping only the pole contribution corresponding to a positive energy for spectator nucleon. We find,

$$F_{m,m'}^0(s, t) = \int \frac{d^3\mathbf{k}}{(2\pi)^3} \frac{\Gamma_{m'}^\dagger(P - k + l) \hat{F}(\hat{s}, t) \Gamma_m(P - k)}{2k_0 [(P - k + l)^2 - m_N^2 + i\epsilon] [(P - k)^2 - m_N^2 + i\epsilon]} \quad (3)$$

$$+ (n \leftrightarrow p).$$

We now make use of the correspondence between the non-relativistic wave function and the vertex function,

$$\tilde{\Psi}_m(\mathbf{k}_{rel}) \equiv \frac{-\Gamma_m(P - k)}{2\sqrt{k_0}(2\pi)^3 D(P - k)}, \quad (4)$$

which is established by the Lippman-Schwinger equation [13] and by demanding that the non-relativistic wavefunction be normalized to unity. Here,  $-D(P - k)$  is the propagator denominator of the struck nucleon. We write  $\mathbf{k}_{rel}$  to indicate that the argument of the wave function is the **relative** 3-momentum of the two nucleons. Using Eq. (3) with Eq. (4) and using lab frame kinematics yields,

$$F_{m,m'}^0(E_\gamma, l) = 2 \int d^3\mathbf{k} \tilde{\Psi}_{m'}^\dagger(\mathbf{k} - \mathbf{l}/2) \hat{F}(E_\gamma, k, l) \tilde{\Psi}_m(\mathbf{k}) + (n \leftrightarrow p). \quad (5)$$

We stress, at this point, that Eq. (5) does **not** coincide with the conventional VMD-Glauber theory because we have abandoned the usual assumptions that allow us to ignore the  $\mathbf{k}$ -dependence in the basic amplitude, which would normally allow us to factor the basic amplitude out of the integral and leave us with the product of the basic amplitude with the non-relativistic form factor. For heavier vector meson's (like the  $\phi$ -meson), the vector meson mass may not be negligible, and the  $\hat{s}$ -dependence of the basic amplitude becomes non-trivial as the threshold energy is approached from above.

### C. The Double Scattering Amplitude

Having obtained the Born term in Eq. (3), we move on to calculate the double scattering term of Fig. 2. Applying the effective Feynman diagrammatic rules, we obtain

$$F_{m,m'}^1(s, t) = - \int \frac{d^4p_s}{i(2\pi)^4} \frac{d^4p'_s}{i(2\pi)^4} \frac{\Gamma_{m'}^\dagger(P + l - p'_s) \bar{F}(\bar{s}, \bar{t}) \hat{F}(\hat{s}, \hat{t}) \Gamma_m(P - p_s)}{[p_s^2 - m_N^2 + i\epsilon] [p'_s{}^2 - m_N^2 + i\epsilon] [(P - p_s)^2 - m_N^2 + i\epsilon]} \quad (6)$$

$$\times \frac{1}{[(P + l - p'_s)^2 - m_N^2 + i\epsilon] [(q - l + p'_s - p_s)^2 - M_V^2 + i\epsilon]} + (p \leftrightarrow n).$$



Figure 2 and Eq. (6) express the following sequence of events: The incident photon scatters from a nucleon with center of mass energy,  $\sqrt{\bar{s}}$ , producing an intermediate state with invariant mass,  $M_V$ . The intermediate state propagates through the deuteron before scattering from the other nucleon with center of mass energy  $\bar{s}$ . (Bars over variables will indicate that they correspond to the secondary scattering.) We neglect fluctuations of the intermediate state for the present purposes.

Now let us integrate over,  $p_{s,0}$  and  $p'_{s,0}$ . The crosses on the spectator nucleon lines in Fig. 2 indicate that we are taking only the poles corresponding to the situation where these two lines are on-shell.

Performing the integrations over  $p_{s,0}$  and  $p'_{s,0}$  and applying the definition in Eq. (4), we recover the formula quoted in [5],

$$F_{m,m'}^1(E_\gamma, l) = - \int \frac{d^3\mathbf{p}_s' d^3\mathbf{p}_s}{(2\pi)^3} \frac{\tilde{\Psi}_{m'}^\dagger(\frac{1}{2} - \mathbf{p}_s') \bar{F}(\bar{s}, \bar{t}) \hat{F}(\hat{s}, \hat{t}) \tilde{\Psi}_m(-\mathbf{p}_s)}{\sqrt{p_{s,0} p'_{s,0}} [(q - l + p'_s - p_s)^2 - M_V^2 + i\epsilon]}. \quad (7)$$

The  $(p \rightarrow n)$  term is implicit in these equations. Finally, we put this equation into a form that makes the next section slightly more manageable by transforming the variables of integration from  $p'_s$  and  $p_s$  to  $p \equiv (p_s + p'_s)/2$  and  $k \equiv p'_s - p_s$ , and we make the redefinitions,  $k \rightarrow k + l/2$ , and  $p \rightarrow p + \frac{l}{4}$ . The result of these changes is:

$$F_{m,m'}^1(E_\gamma, l) = - \int \frac{d^3\mathbf{p} d^3\mathbf{k}}{(2\pi)^3} \frac{\tilde{\Psi}_{m'}^\dagger(\mathbf{p} + \frac{\mathbf{k}}{2}) \bar{F}(\bar{s}, \bar{t}) \hat{F}(\hat{s}, \hat{t}) \tilde{\Psi}_m(\mathbf{p} - \frac{\mathbf{k}}{2})}{m_N [(q + k - \frac{l}{2})^2 - M_V^2 + i\epsilon]} \quad (8)$$

$$+ (p \leftrightarrow n).$$

In Eq. (8), we have given the amplitude a superscript, 1, to distinguish it from the Born term.

We will summarize this section by cleaning up our notation and by writing out the correct expressions for the kinematic variables in terms of the integration variables, taking into account the variable transformations that were needed to get Eqs. (5) and (8). We explicitly expand each expression to linear order in nucleon momentum in the lab frame. Furthermore, we assume that nucleon 3-momentum and the exchanged 3-momentum are both small and of the same order of magnitude relative to all masses involved. Subscripts  $a$  denote Born amplitude quantities while subscripts  $b$  denote double scattering quantities. The variables

in each expression are established in the particular diagram under consideration. First, we have,

$$\begin{aligned}\hat{s}_a &= ((P - k) + q)^2 \\ &= m_N^2 + 2E_\gamma m_N + 2E_\gamma k_z + \mathcal{O}(\mathbf{k}^2).\end{aligned}\tag{9}$$

Recalling the variable transformations we made in the double scattering term and noting that  $\mathbf{p}$ ,  $\mathbf{k}$  and  $\mathbf{l}$  are all of the same order of magnitude, we have,

$$\begin{aligned}\hat{s}_b &= (q + P - p_s)^2 \\ &= m_N^2 + 2E_\gamma m_N + 2E_\gamma \left(p_z - \frac{k_z}{2}\right) + \mathcal{O}(\mathbf{p}^2).\end{aligned}\tag{10}$$

Note that there is only dependence upon  $k_z$  and that  $\mathbf{k}$  contributions come into play only at higher order in nucleon momentum. For the rescattering amplitude, we get,

$$\begin{aligned}\bar{s}_b &= (k_V + p_s)^2 \\ &= M_V^2 + m_N^2 + 2E_V m_N - 2E_\gamma \left(p_z - \frac{k_z}{2}\right) + \mathcal{O}(\mathbf{p}^2).\end{aligned}\tag{11}$$

This last value is obtained after the pole in  $k_z$  is taken, giving the intermediate state an invariant mass of  $k_V^2 = M_V^2$ . The values of  $t$  to be used in each of these cases is,

$$\hat{t}_a = t \tag{12}$$

$$\hat{t}_b = \left(\frac{l}{2} - k\right)^2 = \left(\frac{l_0}{2}\right)^2 + \frac{l_z k_z}{2} - \left(\frac{l_\perp}{2} - k_\perp\right)^2 + \mathcal{O}(\mathbf{k}^2) \tag{13}$$

$$\bar{t}_b = \left(\frac{l}{2} + k\right)^2 = \left(\frac{l_0}{2}\right)^2 - \frac{l_z k_z}{2} - \left(\frac{l_\perp}{2} + k_\perp\right)^2 + \mathcal{O}(\mathbf{k}^2). \tag{14}$$

In the usual VMD-Glauber theory expression for the double scattering term, one keeps only the perpendicular components of  $\hat{t}$  and  $\bar{t}$ . The terms proportional to  $k_z$  are small and since they come with opposite sign, they tend to cancel if the  $t$ -dependence of the basic amplitude is nearly exponential. The terms with  $l_0^2$  are proportional to  $t^2/M_V^2$ . Thus, we continue to neglect both of the first two terms in Eqs. (13) and (14).

By using the kinematic expressions of Eqs. 9 through 14 in Eqs. 5 and 8, we may ensure that the factors multiplying the deuteron wavefunction in each of the integrals is correct to linear order in nucleon 3-momentum (or exchanged 3-momentum).

### III. NUMERICAL ESTIMATES AND THE RELATIONSHIP WITH VMD-GLAUBER THEORY

#### A. Differential Cross Section

Now that we have calculated the Born and Double scattering amplitudes, let us set up notation that allows us to express the total differential cross section in terms of the basic amplitudes for  $\gamma N$  and  $VN$  scattering. For any exclusive two body reaction involving incoming particles of mass  $m_1$  and  $m_2$  and center of mass energy squared,  $s$ , the differential cross section may be represented as follows:

$$\frac{d\sigma^{m,m'}}{dt} = \frac{1}{16\pi\Phi(s, m_1, m_2)} |F_{m,m'}(s, t)|^2, \quad (15)$$

where,

$$\Phi(s, m_1, m_2) \equiv ((s - m_1^2)^2 + m_2^4 - 2sm_2^2 - 2m_1^2m_2^2). \quad (16)$$

In particular, the differential cross section for the reaction in Eq. (1) is,

$$\frac{d\sigma^{m,m'}}{dt} = \frac{1}{16\pi\Phi(s, 0, m_N)} |F_{m,m'}^0(s, t) + F_{m,m'}^1(s, t)|^2. \quad (17)$$

It follows from Eqs. (2) and (8) that the numerical calculations of Eq. (17) will require as input the amplitudes for both the  $\gamma N \rightarrow VN$  and the  $VN \rightarrow VN$  interactions.

To proceed, we obtain a parameterization of the photo-production differential cross section in a form that will provide a smooth transition to the VMD-Glauber regime by writing,

$$\frac{d\hat{\sigma}^{\gamma N \rightarrow VN}}{dt}(\hat{s}, \hat{t}) = \frac{\hat{n}_0^2}{16\pi} \left( \frac{\hat{s}}{\hat{s}_0} \right)^{2(\hat{\alpha}(t)-1)} \hat{f}^2(\hat{t}) \hat{g}^2(\hat{s}, \hat{t}), \quad (18)$$

for the basic  $\gamma N \rightarrow VN$  interaction. In the high energy photon limit, the function  $\hat{f}(\hat{t})$  reduces to the usual exponential dependence,  $e^{\hat{B}\hat{t}/2}$ , with the constant  $\hat{B}$  that is typically used to parameterize experimental data as in, for example, Ref. [1]. The Regge trajectory is  $\hat{\alpha}(t) = \hat{\alpha}'t + \hat{\alpha}_0$ . The factor of  $(\frac{s}{s_0})^{\hat{\alpha}(t)-1}$  is the Regge parameterization obtained in the VMD-Glauber regime and  $\hat{g}(\hat{s}, \hat{t})$  is a function which adjusts for other  $s$  and  $t$  dependence that appears in the near threshold regime, but such that  $\hat{g}(\hat{s}, 0)(\frac{s}{s_0})^{\hat{\alpha}(0)-1}$  reduces to 1 in the high energy photon limit. By substituting Eq. (18) into Eq. (15), we obtain,

$$\hat{F}^{\gamma N \rightarrow VN}(\hat{s}, t) = \hat{n}_0(\hat{s} - m_N^2) \left( \frac{\hat{s}}{\hat{s}_0} \right)^{\hat{\alpha}(t)-1} \hat{f}(t) \hat{g}(\hat{s}, t) (i + \hat{\eta}). \quad (19)$$

The variable,  $\hat{\eta}$ , is a possible real contribution to the amplitude. Because  $P_V \gtrsim 1$  GeV, the parameterization we use for the  $VN \rightarrow VN$  simply takes the diffractive form,

$$\bar{F}^{VN \rightarrow VN}(\bar{s}, t) = \sigma_{VN}(\bar{s})(i + \bar{\eta})\sqrt{\Phi(\bar{s}, m_N, M_V)}\bar{f}(\bar{s}, \bar{t}). \quad (20)$$

The function,  $\bar{f}(\bar{s}, \bar{t})$  reduces to a Regge parameterization,  $(\frac{\bar{s}}{s_0})^{\bar{\alpha}(\bar{t}) - \bar{\alpha}(0)}e^{\bar{B}\bar{t}/2}$  in the VMD regime. By applying the optical theorem to Eq. (20), we see that  $\sigma_{VN}(\bar{s})$  is, indeed, the total  $VN$  cross section. The variable,  $\bar{\eta}$  is a possible real part of the amplitude.

The choice of this peculiar notation is made so that we may smoothly recover the usual Regge parameterizations when we consider the VMD-Glauber approximation. Indeed, applying the VMD hypothesis in the appropriate kinematical regime allows us to assume that  $\hat{F}(\hat{s}, \hat{t}) \propto \bar{F}(\bar{s}, \bar{t})$ . Thus, applying the optical theorem allows one to deduce the  $VN \rightarrow VN$  amplitude. Therefore, we have,

$$\hat{F}(\hat{s}, \hat{t}) \xrightarrow{VMD} \hat{s}\hat{n}_0(i + \hat{\eta})\hat{s}^{\hat{\alpha}'\hat{t}}e^{\hat{B}\hat{t}/2} \quad (21)$$

$$\bar{F}(\bar{s}, \bar{t}) \xrightarrow{VMD} \bar{s}\sigma_{VN}(i + \bar{\eta})\bar{s}^{\bar{\alpha}'\bar{t}}e^{\bar{B}\bar{t}/2}. \quad (22)$$

In this way, we show how our parameterizations reduce smoothly to the expressions obtain within Regge theory and the VMD hypothesis.

One may fit all of the functions that define the expression for  $\hat{F}(\hat{s}, t)$  directly to data for  $\frac{d\sigma_{\gamma N \rightarrow VN}}{dt}$ . The function,  $\hat{g}(\hat{s}, \hat{t})$  has been introduced to account for peaks in the energy dependence or other irregular energy dependence near the threshold. Without the VMD hypothesis, we can assume no relationship between  $\hat{F}(\hat{s}, \hat{t})$  and  $\bar{F}(\bar{s}, \bar{t})$ . Near threshold, therefore,  $\bar{F}(\bar{s}, \bar{t})$  must be obtained from a theoretical model. Conversely, one can use data for the reaction in Eq. (1) to extract  $\bar{F}(\bar{s}, \bar{t})$ .

## B. Corrections to Factorizability and an Effective Form Factor

We now define an effective form factor,

$$S_{eff}^{m, m'}\left(E_\gamma, \frac{1}{2}\right) \equiv \int \frac{d^3\mathbf{k}(\hat{s}_a - m_N^2)}{2E_\gamma m_N} \left(\frac{\hat{s}_a}{2E_\gamma m_N}\right)^{\alpha(t)-1} \hat{g}(\hat{s}, t) \tilde{\Psi}_{m'}^\dagger\left(\mathbf{k} - \frac{1}{2}\right) \tilde{\Psi}_m(\mathbf{k}), \quad (23)$$

for the Born term, and an effective basic amplitude,

$$\hat{F}_{eff}^0(E_\gamma, t) \equiv 2E_\gamma m_N \hat{n}_0(i + \hat{\eta}) \left(\frac{2E_\gamma m_N}{s_0}\right)^{\alpha(t)-1} f(t). \quad (24)$$

If we substitute Eq. (19) into Eq. (5), then the Born amplitude for production from the deuteron is,

$$F_{m,m'}^0(E_\gamma, l) = 2\hat{F}_{eff}^0(E_\gamma, l)S_{eff,a}^{m,m'}(E_\gamma, l/2) + (n \leftrightarrow p). \quad (25)$$

The definition in Eq. (24) takes the form of a general diffractive parameterization obtained when one makes the VMD hypothesis. However, Eq. (25) is correct without any approximations. We have recovered the usual structure of the Born expression - the product of a diffractive basic amplitude with a form factor. The new feature in Eq. (25) is that our effective form factor depends on the energy of the photon. The definitions that we made in Eqs. (23) and (24) ensure that the effective form factor and the effective diffractive amplitude reduce to the usual non-relativistic form factor and the true diffractive basic amplitude in the limit that  $E_\gamma \gg M_V$ :

$$\begin{aligned} S_{eff}^{m,m'}(E_\gamma, l/2) &\xrightarrow{E_\gamma \gg M_V} S^{m,m'}(l/2), \\ \hat{F}_{eff}^0(E_\gamma, l) &\xrightarrow{E_\gamma \gg M_V} \hat{F}^{VN \rightarrow VN}(\hat{s}, t). \end{aligned} \quad (26)$$

The effective form factor tends to undergo enhancement relative to the usual form factor as the photon energy is decreased (see appendix A). Therefore, if one follows the usual methods of Glauber theory and attempts to extract the basic amplitude at small  $-t$  by using a parameterization of the form of diffractive amplitude and the usual non-relativistic form factor, then, according to Eq. (25), one will over estimate the basic amplitude. By following the usual methods of VMD-Glauber theory, one produces a measurement of the *effective* amplitude rather than the true amplitude.

### C. Corrections to Factorizability in Double Scattering

The double scattering term is more complicated due to the fact that, in Eq. (8), the energy dependence cannot easily be factorized out of the integrand. We may rewrite Eq. (8) using Eqs. (23) and (24) as,

$$\begin{aligned} F_{m,m'}^1(E_\gamma, t) = & - \int dk_z \int d^2\mathbf{k}_\perp \int \frac{d^3\mathbf{p}}{(2\pi)^3} \frac{\hat{f}(\hat{t}_b)\bar{f}(\bar{s}_b, \bar{t}_b)\tilde{\Psi}_{m'}^\dagger(\mathbf{p} + \frac{\mathbf{k}}{2})\tilde{\Psi}_m(\mathbf{p} - \frac{\mathbf{k}}{2})}{m_N [(q - k - \frac{l}{2})^2 - M_V^2 + i\epsilon]} \\ & \times \left[ \left( \frac{\hat{s}}{s_0} \right)^{\hat{\alpha}(\hat{t})-1} \sqrt{\Phi(\hat{s}, m_N, 0)\Phi(\bar{s}, m_N, M_V)} \right] \\ & \times \hat{g}(\hat{s}, \hat{t})\hat{n}_0\sigma_{VN}(\bar{s}) (i + \hat{\eta}) (i + \bar{\eta}). \end{aligned} \quad (27)$$

The nonfactorizability of Eq. (27) near threshold comes from the fact that the basic amplitudes and the factors in braces have non-trivial dependence upon the integration variables. We determine that there is no simple reformulation of the integral in Eq. (27) which consistently accounts for corrections linear in momentum. Therefore, we conclude that a direct evaluation is necessary. Note that, though we have set the integral up for a specific parameterization, the analysis applies to any smooth, slowly varying energy dependent basic amplitude. The  $k_z$  integral is determined by expanding the denominator in Eq. (27),

$$\begin{aligned} \left(q + k - \frac{l}{2}\right)^2 - M_V^2 + i\epsilon &\approx 2E_\gamma \left[-k_z + \frac{l_z}{2} - \frac{M_V^2}{2E_\gamma} + (k - \frac{l}{2})_0 + i\epsilon\right] \\ &= 2E_\gamma [-k_z - \Delta + i\epsilon]. \end{aligned} \quad (28)$$

The second line fixes the definition of  $\Delta$ . Notice that by ignoring the term,  $(k - \frac{l}{2})^2/2E_\gamma$ , we have ignored the possibility of contributions from mesons which are far off shell and which correspond to nucleon 3-momenta that are strongly suppressed by the deuteron wavefunction. Furthermore, note that the pole value of  $k_z$  in this approximation only depends on the external variables and is independent of the transverse motion of the nucleons. The resulting double scattering amplitude is then,

$$\begin{aligned} F_{m,m'}^1(E_\gamma, t) &= \int d^2\mathbf{k}_\perp \int \frac{d^3\mathbf{p}}{(2\pi)^2} \int_{-\infty}^{\infty} \frac{dk_z}{(2\pi)} \frac{\hat{f}(\hat{t}_b) \bar{f}(\bar{s}_b, \bar{t}_b) \tilde{\Psi}_{m'}^\dagger(\mathbf{p} + \frac{\mathbf{k}}{2}) \tilde{\Psi}_m(\mathbf{p} - \frac{\mathbf{k}}{2})}{2E_\gamma m_N [k_z + \Delta - i\epsilon]} \\ &\times \left(\frac{\hat{s}}{s_0}\right)^{\hat{\alpha}(\hat{t})-1} \sqrt{\Phi(\hat{s}, m_N, 0) \Phi(\bar{s}, m_N, M_V)} \hat{g}(\hat{s}, \hat{t}) \hat{n}_0 \sigma_{VN}(\bar{s}_b) (i + \hat{\eta}) (i + \bar{\eta}) \\ &\equiv \int d^2\mathbf{k}_\perp \int \frac{d^3\mathbf{p}}{(2\pi)^2} \int_{-\infty}^{\infty} \frac{dk_z}{(2\pi)} \frac{I_{m,m'}(\mathbf{k}_\perp, k_z, \mathbf{p}, s)}{2E_\gamma m_N [k_z + \Delta - i\epsilon]}. \end{aligned} \quad (29)$$

We have gathered all factors apart from the energy denominators in the integrand into a function,  $I_{m,m'}(\mathbf{k}_\perp, k_z, \mathbf{p}, s)$ . Assuming identical protons and neutrons, we get an identical term for the case where the roles of the neutron and proton are inverted. The result of summing two such terms and using  $\Theta(z) + \Theta(-z) = 1$  is,

$$\begin{aligned} F_{m,m'}^1(E_\gamma, t) &= i \int \frac{d^3\mathbf{p} d^2\mathbf{k}_\perp}{2E_\gamma m_N (2\pi)^2} I_{m,m'}(\mathbf{k}_\perp, -\Delta, \mathbf{p}, E_\gamma) \\ &- \frac{1}{\sqrt{2\pi}} \int \frac{d^3\mathbf{p} d^2\mathbf{k}_\perp}{2E_\gamma m_N (2\pi)^2} \int_{-\infty}^{\infty} dz \tilde{I}_{m,m'}(\mathbf{k}_\perp, z, \mathbf{p}, s) \sin(-\Delta z) \Theta(z). \end{aligned} \quad (30)$$

In the VMD-Glauber approximation,  $\Delta \rightarrow 0$  and  $I_{m,m'}(\mathbf{k}_\perp, 0, \mathbf{p}, s)$  is the usual energy independent density matrix, so the first term in Eq. (30) reduces to the traditional Glauber

expression for double scattering and the second term vanishes. The second term is a correction, discussed in Ref. [5] which arises from the non-zero phase shift in the vector meson wave function induced by longitudinal momentum transfer. In the phase shift term, the factor of  $\sin(-\Delta z)$  is itself a correction of order  $k_z$ , so we neglect Fermi motion and energy dependent corrections to  $I_{m,m'}(\mathbf{k}_\perp, 0, \mathbf{p}, s)$  in the phase shift term.

For a real photon, the double scattering term picks out the longitudinal momentum transfer,

$$\Delta = \frac{l_-}{2} + \frac{M_V^2}{2E_\gamma}. \quad (31)$$

Furthermore,  $l_- = -(M_V^2 - t)/2E_\gamma$ , so

$$\Delta = \frac{t + M_V^2}{4E_\gamma}, \quad (32)$$

and we see that  $\Delta$  is indeed negligible at large center of mass energies and small  $t$ . Corrections to the double scattering term, at linear order in momentum, arise from performing the integral in the first term of Eq. (30), and by retaining the phase shift term.

## IV. SAMPLE CALCULATIONS

### A. Cross Section Calculation

It is usually the case that one calculates the charge and quadrupole form factors in the coordinate space formulation of the form factor. This method reduces the formulae to an extremely simple form and allows one to deal simply and directly with polarizations. For the purpose of modifying the basic amplitude, however, such that it has nucleon momentum dependence, we must maintain the momentum space formulation that results from the direct evaluation of the effective Feynman diagrams in Figs. (1,2). This makes the calculation numerically cumbersome, but dealing with polarizations can be simplified if one chooses the axis of quantization along the direction of momentum exchange [3, 14].

In this section we provide some sample calculations by assuming the applicability of the VMD hypothesis. The purpose for doing this is mainly to provide estimates of the sensitivity to non-factorizability rather than because VMD is thought to be appropriate at intermediate energies. We have extracted estimates of the parameters for production of the  $\rho^0$  and  $\phi$  vector mesons from the basic nucleon interaction cross section data appearing in

Ref. [1], and we have made rough estimates of the parameterization of the  $s$  and  $t$ -dependence of these amplitudes (see Sec. A for a description of the parameterizations). For all of our calculations we use the wavefunction obtained from the Paris N-N potential [15].

Another problem begins to emerge very near to the threshold energy: A large fraction of the momentum integrals begins to violate relativistic kinematic constraints. It is likely that the basic amplitudes vary extremely rapidly in these regions of the integral and that expanding in nucleon momentum is not valid (at least to linear order). In order to make progress, a precise understanding of the off-shell amplitudes based on field theory may be necessary. The best we can do for the moment is to estimate the numerical significance of these regions of the integrand. It may be reasonable (given the two-free-nucleon approximation of the deuteron) to assume that the amplitude becomes highly suppressed in those parts of the integral that violate free nucleon kinematic constraints. This is the assumption we make in the following calculations. If the kinematics-violating parts of the integral are significant, then our assumption leads to very large suppression of the cross section. If  $-t$  is small enough that large suppression is seen, then we may conclude that we are considering regions where the expansion to linear order in nucleon 3-momentum is not a good approximation.

We are mainly interested in the  $\phi$ -production cross section which is dominated by natural parity exchange, even at energies close to threshold, due to the OZI rule. However, to demonstrate the consistency of our approach with traditional methods, we consider first the case of the photo-production of  $\rho^0$ -mesons which has been well understood for some time. The basic amplitude for  $\rho^0$ -production is dominated by soft Pomeron exchange at large energies, so that it is constant at high energies, but it undergoes a relatively steep rise at energies near threshold due to meson exchange. The parameterization we use is shown in appendix A. We use a typical slope of  $7.0 \text{ GeV}^{-2}$  for the  $t$ -dependence. Fig. (4) shows the cross section for  $\rho^0$ -production at the high energy of  $E_\gamma = 30.0 \text{ GeV}$ . For comparison, we show data taken at  $12.0 \text{ GeV}$  from Ref. [1, 4]. Reasonable agreement between the data and calculation is consistent with the near energy independence at high energy.

Now we consider the case of  $\phi$ -meson photo-production. At high energy, we use the Regge dependence,  $\alpha(t) = .27t + 1.14$  given in Ref.[1]. The parameterization that we used is described further in appendix A. As noted in Ref. [1], the energy dependence of the  $\phi$ -meson photo-production cross section is very weak, and the current state of experimental data is still ambiguous as to how much this energy dependence continues close to the threshold. However,



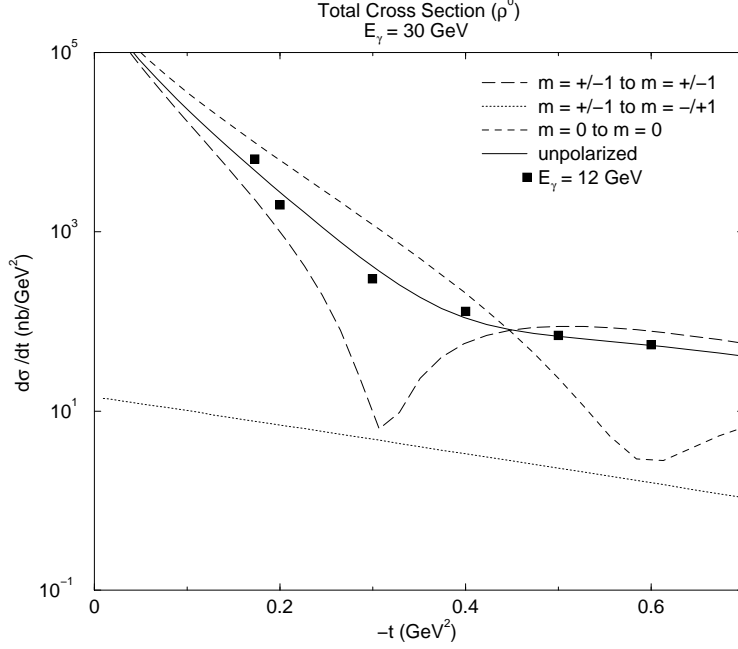


FIG. 4: The unpolarized differential cross section for coherent  $\rho^0$ -meson production compared with the total cross section for different polarizations. The calculation is done with the large photon energy  $E_\gamma = 30$  GeV, and the data for  $E_\gamma = 12$  GeV is taken from Ref. [1].

the large negative ratio of the real to imaginary part of the amplitude ( $\eta = -.48$ ) [16] suggests that some mechanism other than soft Pomeron exchange is significant. This value of the ratio of the real to imaginary part of the  $\phi$ -meson cross section has large error bars and was calculated neglecting longitudinal momentum transfer. However, it is the only measurement we know of at the moment so we use it for the purpose of demonstration. At photon energies near to threshold, the energy dependence of the basic cross section becomes highly non-trivial as observed in Ref. [17]. The results of the calculation done with different deuteron polarizations with each term shown explicitly are shown for a photon energy of  $E_\gamma = 30.0$  GeV in Fig. 5 and for a photon energy of  $E_\gamma = 3.0$  GeV in Fig. 6. Note that there is no contribution from the Born term for the  $m = +/ - 1$  to  $m = -/ + 1$  transition. The result is summarized in Figs. 7 and 8 which show the differential cross section for different polarizations along with the unpolarized cross section for photon energies of 30.0 GeV and 3.0 GeV respectively.

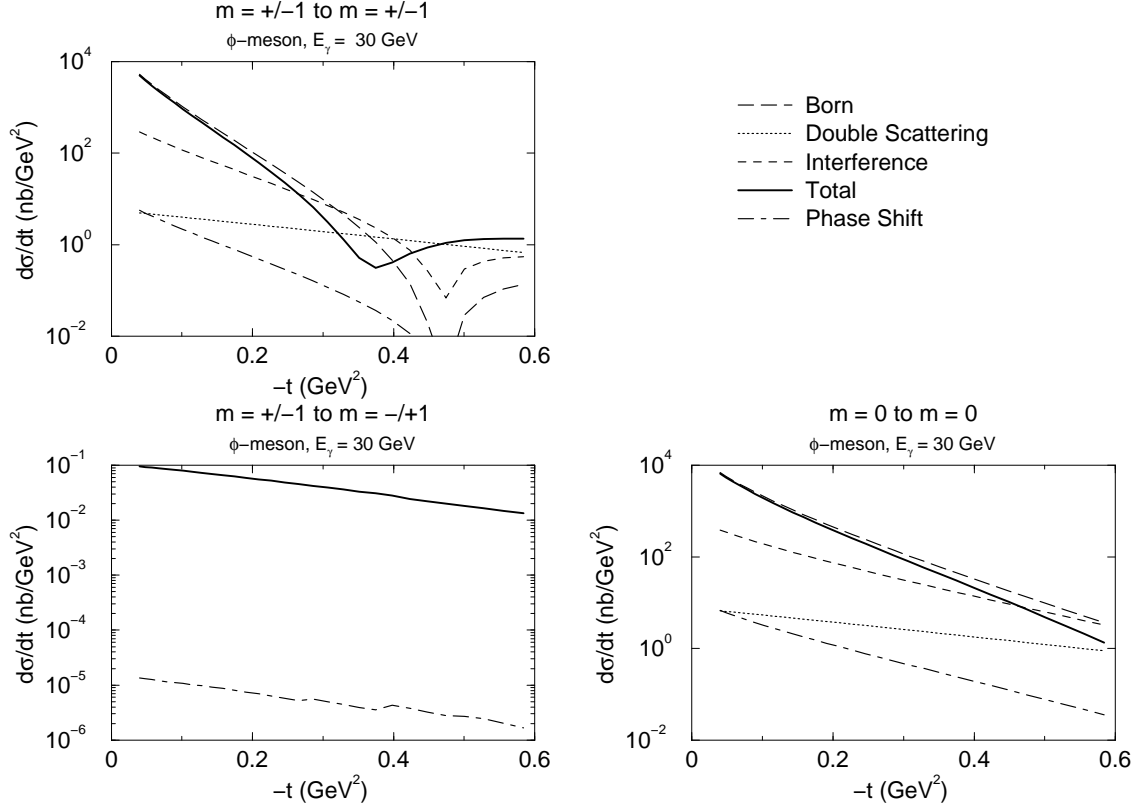


FIG. 5: The long-dashed, dotted, dashed, solid, and dot-dashed lines refer to the Born, double, interference, total, and phase shift terms respectively for a photon energy of  $E_\gamma = 30.0$  GeV. For the spin flip cross section, the only non-zero contribution comes from the double scattering term. Note the different scale on the axis for the spin-flip contribution.

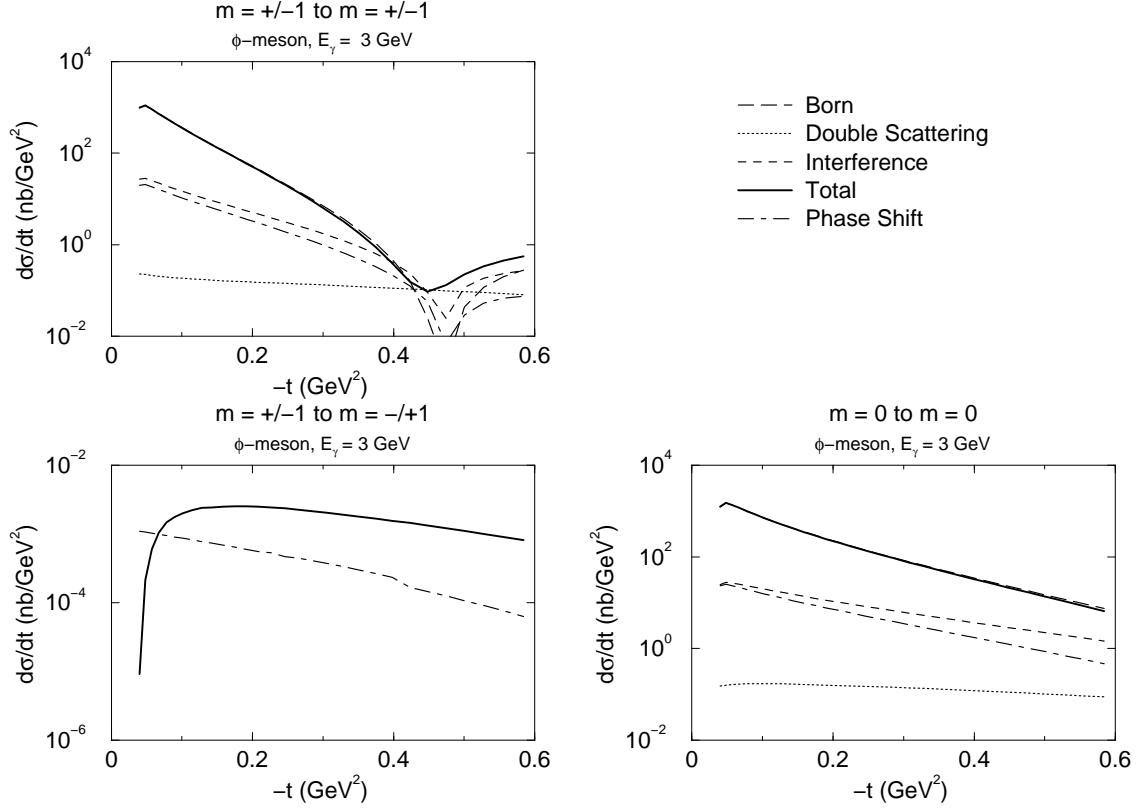


FIG. 6: The long-dashed, dotted, dashed, solid, and dot-dashed lines refer to the Born, double, interference, total, and phase shift terms respectively for a photon energy of,  $E_\gamma = 3.0$  GeV. For the spin flip cross section, the only non-zero contribution comes from the double scattering term. Note the different scale on the axis for the spin-flip contribution.

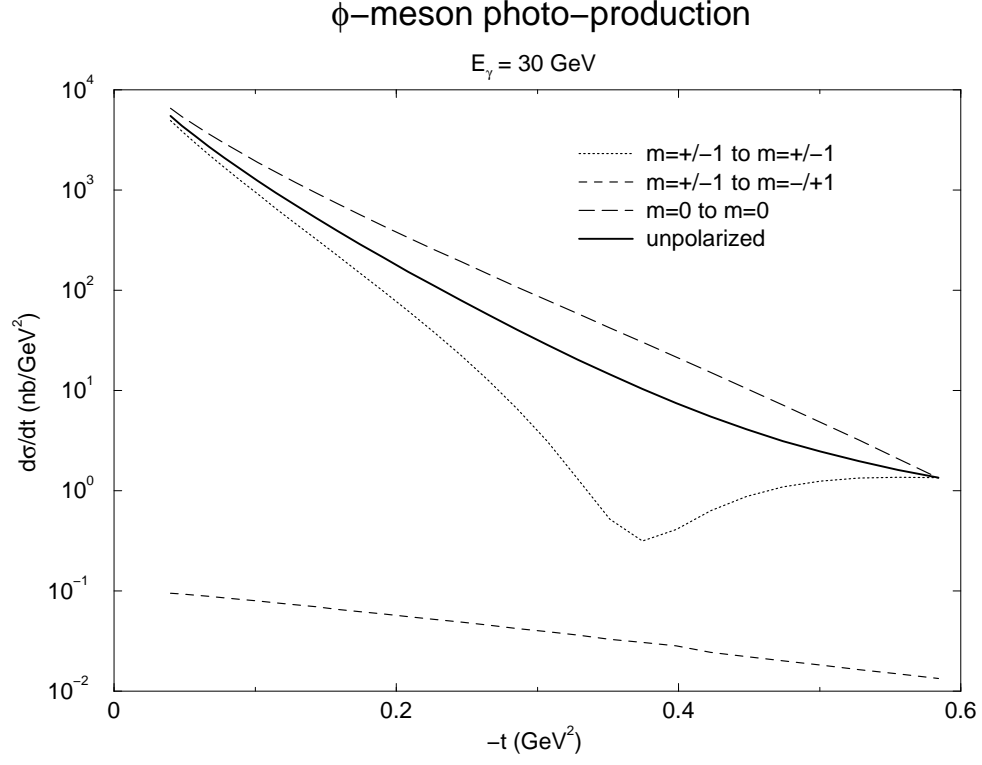


FIG. 7: The differential cross section for  $\phi$ -meson production for different polarizations for a photon energy of  $E_\gamma = 30.0 \text{ GeV}$ .

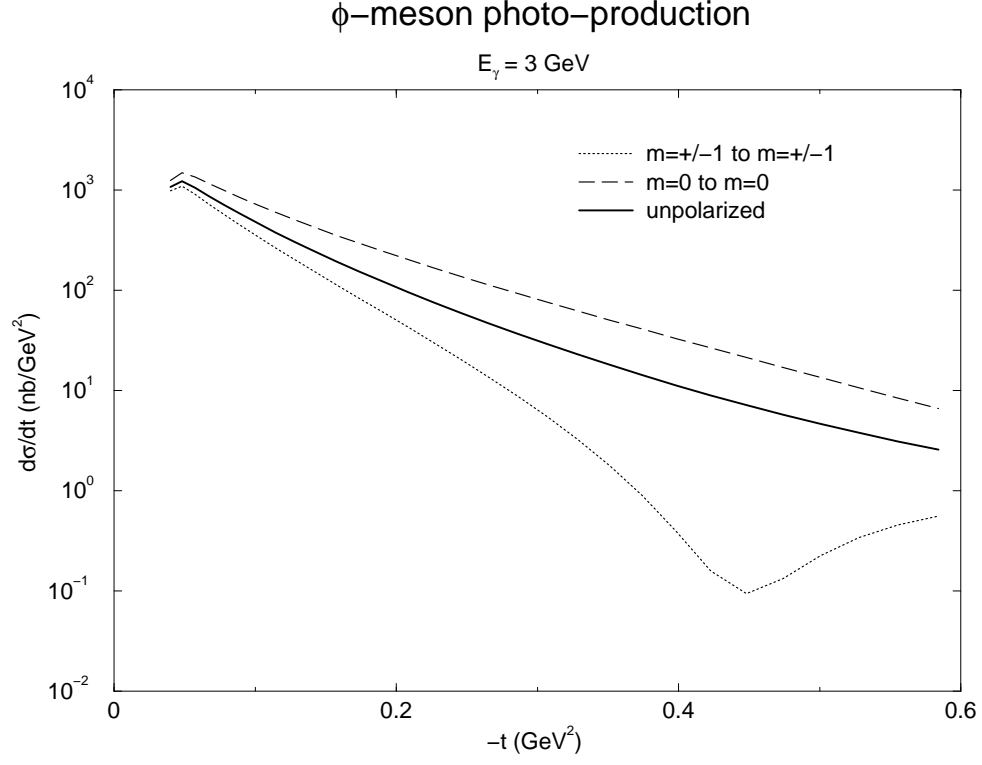


FIG. 8: The differential cross section for  $\phi$ -meson production for different polarizations For a photon energy of  $E_\gamma = 3.0 \text{ GeV}$ . The deuteron spin flip term is negligible at these energies.

Next we plot the total unpolarized cross section as a function of photon energy for a range of fixed values of  $-t$ . This allows us to compare the factorized and unfactorized calculations and to determine approximately at what value of energy the transition to the VMD-glauber regime occurs. We note several features of the  $\gamma D \rightarrow \phi D$  cross section: The double scattering term contributes less in the case of low energy scattering relative to the Born term than in the high energy case. In the low energy case,  $E_\gamma = 3.0$  GeV, we see that the differential cross section begins to curl downward. This is an indication, as discussed earlier in this section, that a significant region of the integrand violates relativistic kinematics and has been set equal to zero. Thus, the region at small  $-t$  that begins to curl downward signals the region where our linear order approximation is no longer necessarily valid.

We remark that the effect of Fermi motion on the  $\rho^0$ -meson cross section is small (less than about 10 percent) for the whole range of energies under consideration and for both large and small  $-t$  (See Figs. 9 and 10). However, for low energies, the effect of Fermi motion on the  $\phi$ -meson cross section is not negligible as seen in Figs. 11 and 12. There is nearly a 30 percent suppression of the factorized cross section relative to the unfactorized cross section at the lowest energy (3.0 GeV) in Fig. 12. In Fig. 11 we see that the unfactorized cross section becomes suppressed at the lowest energy due to the nearness of  $-t$  to  $-t_{min}$ . However, as we have seen, the calculation is somewhat questionable in the very small  $-t$  and  $E_\gamma$  regime.

One must also be careful in extracting the total  $\phi N$  cross section from the  $\gamma D \rightarrow \phi D$  differential cross section at large  $-t$  where the double scattering term dominates. The amplitude for scattering from a polarized deuteron, from  $m = +/ - 1$  to  $m = +/ - 1$ , is plotted in Fig. 13 where the result of using a typical value for the total  $\phi N$  cross section ( $\approx 11$  mb) is compared with the case when the  $\phi N$  cross section is enhanced by a factor of three. Even with the suppression of the double scattering curve that results from Fermi motion, the dip in the cross section is observed to flatten out when the basic  $\phi N$  cross section is large.

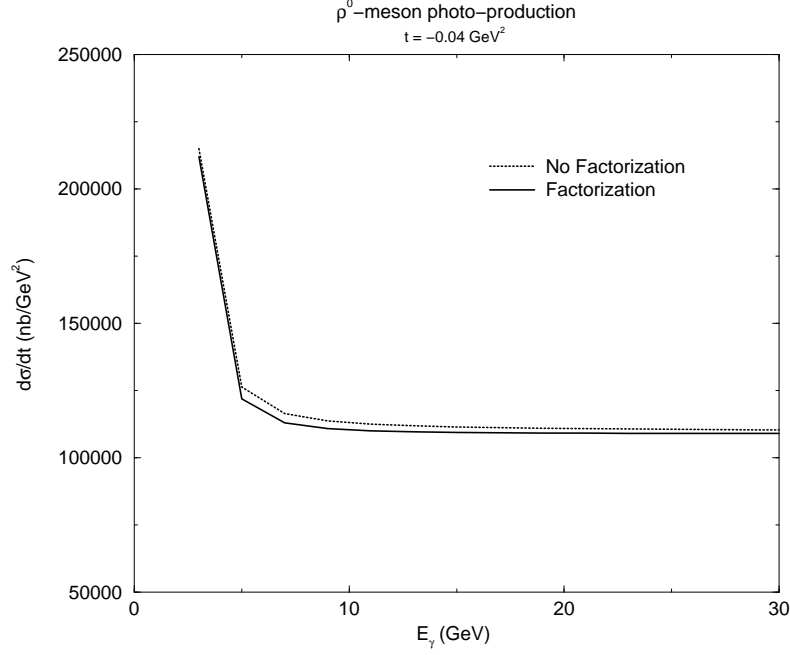


FIG. 9: The energy dependence of the unpolarized differential cross section for  $\rho^0$ -meson photo-production for  $t = -.04 \text{ GeV}^2$ .

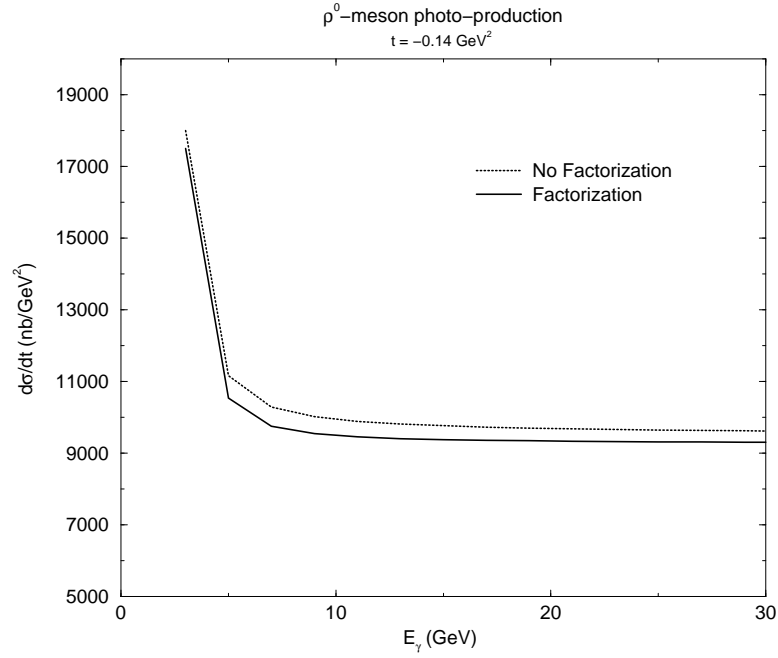


FIG. 10: The energy dependence of the unpolarized differential cross section for  $\rho^0$ -meson photo-production for  $t = -.14 \text{ GeV}^2$ .

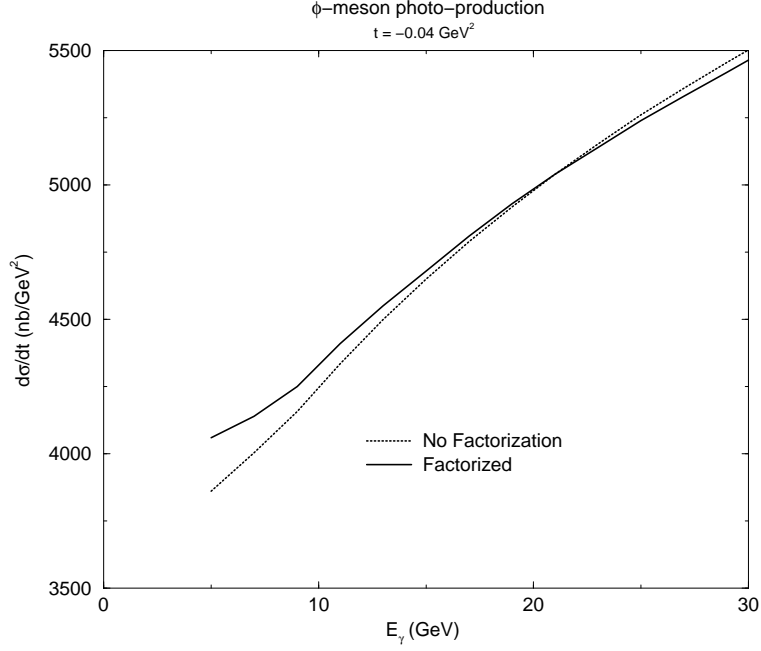


FIG. 11: The energy dependence of the unpolarized differential cross section for  $\phi$ -meson photo-production for  $t = -.04 \text{ GeV}^2$ .

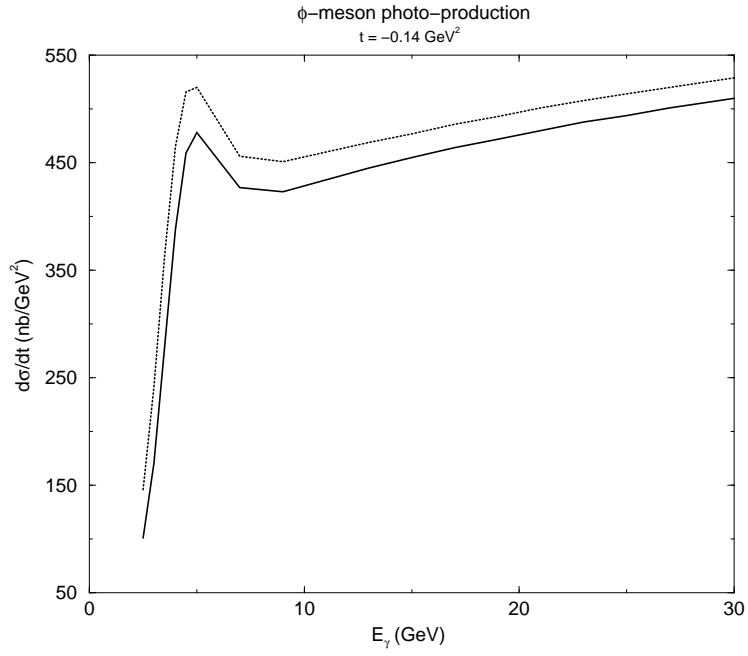


FIG. 12: The energy dependence of the unpolarized differential cross section for  $\phi$ -meson photo-production for  $t = -.14 \text{ GeV}^2$ .



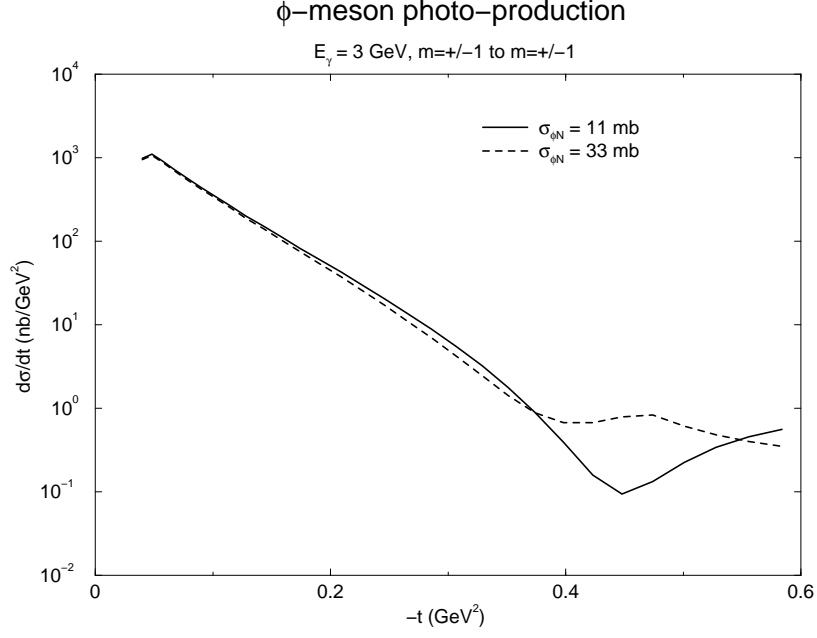


FIG. 13: The energy dependence of the  $m = +/ - 1$  to  $m = +/ - 1$  differential cross section for  $\phi$ -meson photo-production with  $E_\gamma = 3 \text{ GeV}$ . The dashed curve shows the result of increasing the typical basic  $\phi N$  cross section by a factor of 3.

## B. The Problem of Bound State Amplitudes

We have treated the struck nucleon as being on-shell which is consistent with the neglect of terms quadratic in nucleon momentum. However, immediately at the threshold for particle production, the basic amplitude has very unpredictable behavior which may be modified significantly when the nucleon is in a bound state. This is especially clear when we realize that for a given photon energy  $-t_{min}$  is different for a deuteron and an on-shell nucleon target. We cannot predict the effects of the off-shellness of the bound nucleon without a complete, relativistic understanding of the basic amplitude. However, we hope to make predictions in the region of kinematics where it is reasonable to assume that the bound state amplitude is the same as that of the free nucleon amplitude.

In this subsection we discuss rough a way to test the validity of the on-shell amplitude approximation. We do this in the next few paragraphs by directly comparing the amplitude when it is evaluated at the value of  $t_{min}$  for the deuteron with the case when it is evaluated at  $t_{min}$  for a free nucleon with  $s$  given by the exact expression for  $\hat{s}$ ,

$$\hat{s} = 2E_\gamma \left( M_D - \sqrt{m_N^2 + \mathbf{k}^2} + k_z \right) + \left( M_D - \sqrt{m_N^2 + \mathbf{k}^2} \right)^2 - \mathbf{k}^2. \quad (33)$$

The value of the nucleon 3-momentum thus parameterizes the off-shellness of the bound nucleons.  $t'_{min}$  will denote the lower bound of  $-t$  for the free nucleon, whereas  $t_{min}$  is the lower bound of  $-t$  for the deuteron. The struck nucleon inside the deuteron for the unprimed case has  $\hat{s}$  given by Eq. (33). We will now consider the case of a free nucleon, with the same  $\hat{s}$  as for the bound nucleon, but with the nucleon on-shell (i.e.  $k^2 = m_N^2$ ) and with a fixed value for  $k_z$ . So that the free nucleon energy corresponds to the bound nucleon energy, we will continue to use  $M_D - \sqrt{m_N^2 + \mathbf{k}^2}$  for the energy of the struck nucleon. In short, we are comparing  $t_{min}$  for  $\gamma$  scattering off a deuteron with  $t'_{min}$  for  $\gamma$  scattering off a free nucleon, with energy corresponding to that of the bound nucleon in both cases.

We expect the rate of variation of the basic amplitude with  $t$  to be very large near  $t_{min}$ . If there is a significant contribution to the integral in Eq. (5) from regions near  $t_{min}$ , then  $t_{min}$  should nearly equal  $t'_{min}$  in order to make the on-shell amplitude a valid approximation to the bound state amplitude. We can use the difference between these two values of  $t_{min}$  to estimate the effect of the off-shellness on the the amplitude.

In order to test the effect of the off-shellness of the basic amplitude, we consider two

extremes. First, the bound state basic amplitude could be evaluated at the physical value of  $t$  for the photon-deuteron process. That is, we could calculate the amplitude,  $\hat{F}(\hat{s}, t)$  at  $t$  where  $t$  is the physical value of  $t$  for the photon deuteron process. In this case, since  $t_{min}$  is smaller for the deuteron than  $t'_{min}$  is for the nucleon, then we are probably overestimating the cross-section. On the other hand, we could evaluate the basic amplitude at  $F(\hat{s}, t - (t_{min} - t'_{min})) = F(\hat{s}, t - \Delta t)$  where  $t'_{min}$  is the minimum  $t$  for the free, on-shell nucleon. With this second method for choosing which value of  $t$  to use in the basic amplitude, the basic amplitude behaves like the free, on-shell nucleon amplitude in the region of  $t$  close to  $t_{min}$ . Hence, with this method, we are probably underestimating the value of the basic amplitude. In the high energy limit,  $\Delta t$  vanishes and the two amplitudes are equal, and the difference between the two provides an estimate of the off-shell effects. (Note that we must specify a value for  $\mathbf{k}$  in order to make a comparison.) Any amplitude which has a relatively slow and smooth variation with  $t$  will yield a small difference between  $\hat{F}(\hat{s}, t)$  and  $F(\hat{s}, t - \Delta t)$ . We made this comparison for  $\phi$ -meson production with the parameterization in appendix A and we find only a few percent deviation. We conclude that at a few GeV above threshold it is reasonable to continue using the on-shell amplitude of the nucleon. This approximation was made assuming that the  $t$ -dependence is relatively weak and varies smoothly. Surely extremely near to threshold, off-shellness effects will become significant, but we hope this argument supports making kinematical corrections as a first approximation as one gets closer to the threshold energy.

## V. SUMMARY AND CONCLUSIONS

The main conclusion of this paper is that the effect of factorization break-down is significant for intermediate energies. We have outlined the steps one must follow in order to obtain corrections to leading order in the bound nucleon momentum. We have shown (see Fig. 12) that, away from  $t = t_{min}$ , ignoring Fermi motion can lead to a significant over estimate of basic cross sections extracted from  $\gamma D \rightarrow \phi D$  cross section data. This effect will certainly need to be taken into account in future searches for new production mechanisms near threshold. Furthermore, we observe that the contribution from double scattering is numerically suppressed relative to the Born approximation as one approaches the threshold. This probably leads to  $A$ -dependence of the cross section that is much less trivial than the

$A^{1/3}$  dependence prescribed by traditional Glauber theory. Hence, there will need to be a revision in efforts to extract basic cross sections from nuclear data using extrapolations in  $A$ . We note that data given in Ref. [18] predicts a very high  $\phi N$  total cross section using the traditional Glauber approach. The next step will be to determine how the non-factorization effects discussed in this paper affect a Glauber series in incoherent scattering and so see how much it changes the prediction of a large basic cross section.

We have purposefully over-simplified our analysis here for the purposes of demonstration. In particular, we have applied the VMD hypothesis at energies where it is suspect and we have neglected fluctuations and  $\omega - \phi$  mixing in the intermediate vector meson in the double scattering term. Further analysis will need to include these effects. In order made further numerical progress, we will need firmer parameterizations of the basic cross sections for vector meson production from nucleons including an over all normalizations. The current set of experimental data allows too much freedom in the parameterizations near threshold. For theoretical work, it would be useful for the purposes of comparison to have a widely agreed upon set of parameterizations.

Furthermore, we will need a complete understanding of the off-shell amplitudes if we are to take into account the higher order momentum corrections that will be necessary just at the threshold, though we have argued that the for smoothly varying basic cross sections, the effect of off-shell amplitudes is small relative to the effect correction to linear order in nucleon momentum.

## Acknowledgments

T.C. Rogers would like to thank Steve Hepelmann for useful discussions, Nick Conklin and Isaac Mognet for sharing their computers to help with calculations, and David Landy for finding typos. Feynman graphs were made using Jaxodraw [12].

## APPENDIX A: PARAMETERIZATIONS

Here we describe the fits of the basic  $\gamma N \rightarrow \phi N$  cross section that we used for our sample calculations. The object here is not necessarily to produce accurate parameterizations, but rather to devise parameterizations that demonstrate the effects of Glauber factorization

while being consistent with recent and established experimental results.

First we consider the  $\gamma N \rightarrow \rho^0 N$  differential cross section. For this we use a simple exponential  $t$ -dependence with a typical exponential slope of  $B = 7.0 \text{ GeV}^{-2}$  and an overall normalization of  $105 \mu b/\text{GeV}^2$ . (See, e.g. Ref. [1].) It is known that at low energies the normalization undergoes a steep rise. We take this into account in our calculation by including a factor of  $(1 + \frac{a}{E_\gamma^4})$  in the overall normalization and then doing a least squares fit to obtain the parameter,  $a$ . The result is shown in Fig. 14. As seen in the main part of the text, the variation is too weak to have a very large effect on the final differential  $\gamma D \rightarrow \rho^0 D$  cross section.

The case of the  $\phi$ -meson is more complicated due to the irregular behavior near threshold. The normalization of the low energy data, taken from recent LEPS data in Ref. [17], is obtained from an effective Pomeron and pseudo-scalar exchange model [19]. The high energy parameterization was obtained in Ref. [1] by fitting a diffractive-like cross section to a large set of experimental data. We want to interpolate quickly but smoothly between the low energy and high energy data. There is an exponential factor,  $e^{Bt}$ , associated with both the high and the low energy behavior, but the slope,  $B$ , is around  $3.4 \text{ GeV}^{-2}$  for the low energy behavior ( $E_\gamma \lesssim 4.0 \text{ GeV}$ ) while it is around  $4.8 \text{ GeV}^{-2}$  for the high energy behavior. Thus, for the exponential slope we use,

$$B(E_\gamma) = 4.8 - (4.8 - 3.4)e^{-0.001E_\gamma^4} \text{ GeV}. \quad (\text{A1})$$

Next, for the low energy region, there is no Regge slope. That is,  $\alpha' = 0$  in the factor,  $s^{\alpha't}$ . But, in the high energy region,  $\alpha' = .27 \text{ GeV}^{-2}$ . Thus, we use,

$$\alpha'(E_\gamma) = .27 \text{ GeV}(1 - e^{-.001E_\gamma}). \quad (\text{A2})$$

Now we consider the behavior of  $\frac{d\sigma}{dt}|_{t=0}$ . The parameterization in Ref. [1] is

$$\left. \frac{d\sigma}{dt} \right|_{t=0} = 1.34 s^{.28}, \quad (\text{A3})$$

and over-all units will be understood to be  $\frac{\mu b}{\text{GeV}^2}$ . In order to match to the data of Ref. [17] we want a peak to appear at around  $E_\gamma = 2.0 \text{ GeV}$ . Therefore, we adjust the parameterization to,

$$\left. \frac{d\sigma}{dt} \right|_{t=0} = 1.34 s^{.28} (1 + a e^{-b(E_\gamma - c)^2}). \quad (\text{A4})$$

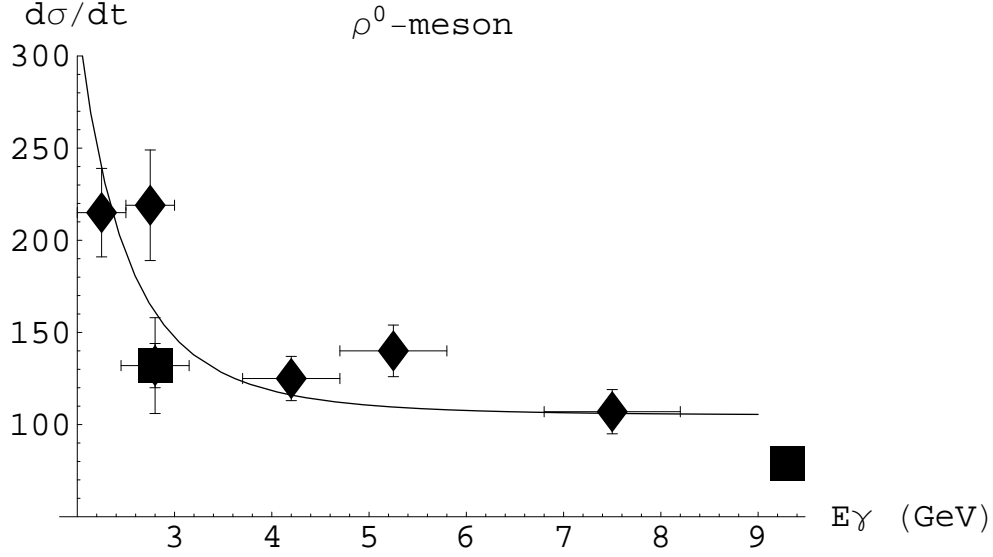


FIG. 14: We obtain this fit using data from Ref. [20, 21, 22] (listed in Ref. [1]). We use an inverse-fourth function at low energies and apply a least-squares fit.

We use Eq.(A4) to fit to the low energy data of Ref. [17] while assuring that the high energy parameterization of Eq.(A3) is reproduced at high energies. We note, finally, that the low energy data is actually give for  $t = t_{min}$  rather than  $t = 0$ . Therefore, we must be sure to include a factor of  $e^{B(E_\gamma)t_{min}}$  in the final result for  $\frac{d\sigma}{dt}_{t=0}$ . The result of our parameterization for  $\frac{d\sigma}{dt}_{t=0}$  for the  $\phi$ -meson is shown in Fig. 15.

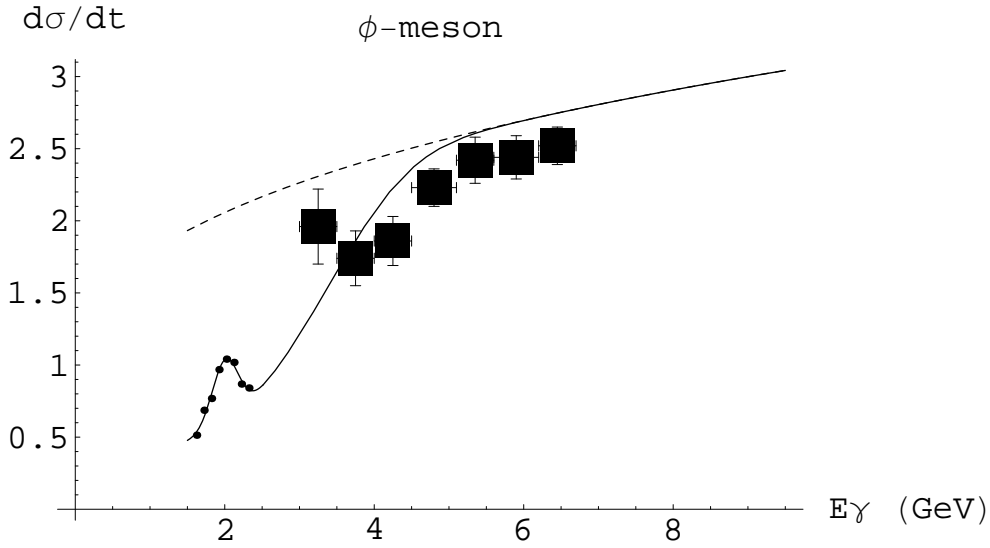


FIG. 15: The low energy data here is from Ref. [17]. The curve at high energies was taken from Ref. [1]. The dashed curve shows its extension to lower energies. The high energy data is taken from Ref. [23] and is presented to establish the consistency of the high energy parameterization. The curve at low energies has been fit to the low energy data of Ref. [17] using a least-squares fit.

- 
- [1] T. H. Bauer, R. D. Spital, D. R. Yennie and F. M. Pipkin, Rev. Mod. Phys. **50**, 261 (1978) [Erratum-ibid. **51**, 407 (1979)].
  - [2] R.P. Feynman “The Nucleon-Nucleon Interaction” Addison Wesley Longman, Inc., 1972.
  - [3] V. Franco and R. J. Glauber, Phys. Rev. **142**, 1195 (1966).
  - [4] R.L. Anderson *et al.*, Phys. Rev. D **4**, 3245 (1971); I.D. Overman, Ph.D. thesis, SLAC-140, UC-34, 1971.
  - [5] L. Frankfurt, G. Piller, M. Sargsian and M. Strikman, Eur. Phys. J. A **2**, 301 (1998).
  - [6] A. I. Titov, T. S. Lee, H. Toki and O. Streltsova, Phys. Rev. C **60**, 035205 (1999).
  - [7] A. I. Titov, M. Fujiwara and T. S. H. Lee, Phys. Rev. C **66**, 022202 (2002) [arXiv:nucl-th/0207079].
  - [8] Y. s. Oh, J. Korean Phys. Soc. **43**, S20 (2003) [arXiv:nucl-th/0301011].
  - [9] L. L. Frankfurt and M. I. Strikman, Nucl. Phys. B **250**, 143 (1985).

- [10] L. L. Frankfurt, W. R. Greenberg, G. A. Miller, M. M. Sargsian and M. I. Strikman, Z. Phys. A **352**, 97 (1995)
- [11] L. L. Frankfurt, M. M. Sargsian and M. I. Strikman, Phys. Rev. C **56**, 1124 (1997);  
M.M. Sargsian, Int. J. Mod. Phys. E **10**, 405 (2001).
- [12] D. Binosi and L. Theussl, Comput. Phys. Commun. **161**, 76 (2004) [arXiv:hep-ph/0309015].
- [13] G.E. Brown and A.D. Jackson “The Nucleon-Nucleon Interaction” North-Holland Publishing Company, 1976.
- [14] V. Franco and R. J. Glauber, Phys. Rev. Lett. **22**, 370 (1969).
- [15] M. Lacombe, B. Loiseau, J. M. Richard, R. Vinh Mau, J. Cote, P. Pires and R. De Tourreil, Phys. Rev. C **21**, 861 (1980).
- [16] H. Alvensleben *et al.*, Phys. Rev. Lett. **27**, 444 (1971).
- [17] T. Mibe *et al.* [LEPS Collaboration], arXiv:nucl-ex/0506015.
- [18] T. Ishikawa *et al.*, Phys. Lett. B **608**, 215 (2005).
- [19] A. I. Titov and T. S. H. Lee, Phys. Rev. C **67**, 065205 (2003) [arXiv:nucl-th/0305002].
- [20] J. Ballam *et al.*, Phys. Rev. D **5**, 15 (1972).
- [21] Y. Eisenberg, B. Haber, E. Kogan, E. E. Ronat, A. Shapira and G. Yekutieli, Nucl. Phys. B **42**, 349 (1972).
- [22] J. Ballam *et al.*, Phys. Rev. D **7**, 3150 (1973).
- [23] H. J. Behrend *et al.*, Nucl. Phys. B **144**, 22 (1978).